

# Pressure Sensor Systems for Wide Pressure Ranges Integrated by a Combined CMOS- and MEMS-Technology

Wolfgang Schreiber-Prillwitz<sup>1</sup> and Reinhart Job<sup>2</sup>

<sup>1</sup>ELMOS Semiconductor AG, 44227 Dortmund, Germany

<sup>2</sup>Muenster University of Applied Sciences, Electrical Engineering and Computer Science, 48565 Steinfurt, Germany  
e-mail: reinhart.job@fh-muenster.de

## ABSTRACT

Monolithic integrated pressure sensor systems are realized by the combination of two different technologies: CMOS-technology for the electrical part and MEMS-technology for the pressure sensor part. The paper describes the modification of such pressure sensor systems to extend their original nominal pressure range from 600 mbar to the low pressure range of 40 mbar by keeping a sufficient signal to noise ratio and without changing the original mask set. The general methodology is described, and a comparison between theoretical signal evaluation and measurement is given. The study concentrates on the aspect of the different piezocoefficients for various Boron doping concentrations of the piezoresistors.

**Index Terms:** Pressure Sensor Systems, CMOS Technology, MEMS Technology.

## I. INTRODUCTION

The demands on pressure sensors are multifaceted and requirements on their performances are steadily increasing because of rapidly growing applications fields. Concerning wide spread applications monolithic integrated pressure sensor systems based on the piezoresistive effect in silicon are favorable in most cases. Such systems are equipped with on-chip integrated signal processing and offer great flexibility for numerous detection purposes. Hence, these pressure systems are strongly demanded from the market. Having resilience in mind, their benefit is that no wire bonding between the sensing and circuitry components is required, and therefore, failure due to breaking bond wires is avoided. Since bond pads and a certain frame around the sensing membrane for assembly are omitted, the area around the membrane can be used for circuitry. In general such pressure sensor systems offer amplified output signals, which provide an enhanced robustness against electromagnetic compatibility (EMC) disturbances during transmission. Also calibrated output signals concerning sensitivity, linearity, and temperature dependent effects are usually provided.

The fabrication of pressure sensor systems with on-chip integrated signal processing requires the application of two different technological approaches, which have to be co-integrated, i.e. CMOS technology for the electrical part and MEMS technology for the

pressure sensor part. In the sequence of the technological fabrication process CMOS processing is performed first, then subsequent micromachining is employed for the membrane fabrication.

Economic boundary conditions demand the fabrication of families of pressure sensor systems which cover as wide pressure ranges as possible with changeless lateral membrane geometry, since minimal mask numbers for the CMOS process are aspired. Another important point comes up, if integrated pressure sensor systems for automotive applications are considered. For such applications the CMOS part has to be processed in an automotive qualified standard process, which is very strict with regard to reliability. Changes in the CMOS part – caused for instance by varying membrane geometry – would require a new process qualification, driving development costs often unacceptable high.

Having this background in mind, our investigation was motivated by the extension of a commercial monolithic integrated pressure sensor family with on-chip signal processing towards as wide pressure ranges as possible without changing the lateral pressure membrane geometry; off course, thickness variations of the membrane were possible. The development engineering was carried out in three steps, which were in parts recently separately published [1-3]. First the methodological approach was developed and verified for a sensor family covering four pressure ranges (0 – 1

bar, 0 – 3 bar, 0 – 10 bar, 0 – 30 bar), without lateral change of the membrane geometry [1]. The theory of piezoresistivity for crystalline silicon was applied, combined with finite element analysis of the mechanical stress within the investigated silicon membranes. And the feasibility of the method was shown by comparing simulated bridge signals with measured ones. This was basically the fundament of the development engineering and the whole investigation. In a second step the impact of constraints and process fluctuations was analyzed [2] to get a feeling about the limits of the developed method. The goal was to cover a large pressure range always achieving a sufficient Wheatstone bridge signal for the given signal conditioning as well as a robust mechanical stability of the membrane against pressure overload. Finally, the methodology was used to upgrade the sensor family performance especially also towards lower pressure ranges without strong sensitivity break-down briefly discussed already in [3]. In present publication, we especially concentrate on the latter aspect. We focus on the extension of an already developed monolithic integrated sensor system – designed for wide pressure ranges between about 1.000 hPa (1 bar) and 30.000 hPa (30 bar) – towards significant lower pressure ranges. After the explanation of the developed methodology, we will show that pressure sensor systems for strongly reduced pressure ranges can be achieved, when the variation of the piezocoefficients for different Boron doping concentrations of the piezoresistors is taken into account. After the model of Kanda [4], the relative piezocoefficient is significantly altered by the doping concentration, resulting in higher values for relatively low doping concentrations in the range of  $1 \times 10^{18} \text{ cm}^{-3}$ , and lower values for about  $1 \times 10^{20} \text{ cm}^{-3}$ . Hence, replacing for the piezoresistors on the membrane the typically used boron implantation concentration of  $1 \times 10^{20} \text{ cm}^{-3}$  by a lower one of about  $2.5 \times 10^{17} \text{ cm}^{-3}$  raises the piezocoefficient by a factor of 4, resulting in a higher bridge signal, and with therefore a higher sensitivity. We will discuss in this paper that by a modification of the membrane thickness and a reduction of the boron concentration within the piezoresistors, the measurement range of the sensor system can be extended. In particular, we extended the pressure range from originally 600 hPa down to a low pressure region of about 50 hPa for a given and unchanged lateral membrane geometry and resistor locations.

## II. METHOD AND DATA COLLECTION

For piezoresistive pressure sensors systems, the task of signal evaluation is a standard procedure. In many cases, self-written programs are widely used beside (or even instead of) commercial tools. For the development engineer, the advantage of self-written pro-

grams is the transparency of the methods. In particular, parameter variations or certain conditions can easily be analyzed with regard to the impact on the employed model. And furthermore, appropriate parameters can be easily implemented and compared with experimental analyses.

The studied product family of co-integrated pressure sensor systems is based on the piezoresistive principle in silicon. Piezoresistors are implemented at the membrane edge. As customary, they are wired in Wheatstone bridge configuration to get a good signal output. The relation between piezoresistance and applied stress is given according to Tufte [5] by

$$R/R_0 = \pi_l \times \sigma_l + \pi_t \times \sigma_t \quad (1)$$

where  $\sigma_l$  and  $\sigma_t$  are the longitudinal stress values (i.e. with a parallel alignment of current and stress) and transverse stress values (i.e. with a perpendicular alignment of current and stress) along the according resistors of the bridge;  $\pi_l$  and  $\pi_t$  are the corresponding piezoresistive coefficients, respectively. In the actually used coordinate system the resistors are oriented with their length parallel to the x-axis, and their width along the y-axis, respectively. Therefore, the normal stress  $\sigma_{xx}$  equals  $\sigma_l$  and  $\sigma_{yy}$  equals  $\sigma_t$ .

The developed methodological approach implies five steps: i) one has to build up the 3-dimensional geometry of the device, ii) the finite element analyses (FEA) model has to be built up considering meshing, constraints and pressure loads, respectively; iii) the mechanical stress distributions have to be calculated within the membrane, and the normal stress  $\sigma_{xx}$ ,  $\sigma_l$  and shear stress  $\sigma_{xy}$  values have to be estimated; iv) the mechanical stress has to be converted into electrical signals on base of the real doping profiles, where the piezocoefficients can be deduced from the dopant concentrations; and v) the experimental verification has to be carried out. The signal evaluations start with a simulation of the membranes deflection under pressure load. For this the FEA tool ANSYS® is used, which delivers normal stress values  $\sigma_{xx}$ ,  $\sigma_{yy}$ , and the shear stress  $\sigma_{xy}$ . Fig. 1 shows partitioning details of the employed model and a general view of the structure and meshing. Fig. 1 a) shows details of the partitioning of the geometry of the employed model. The local part of the mesh where the membrane is connected to the base silicon is more finely defined to achieve accurate and reliable peak stress values. Fig.1 b) shows a general view of the structure and the meshing. Simulations were performed using anisotropic (orthotropic) properties for the Young modulus  $E$  and the Poisson ratio  $\nu$  for silicon [5] (Table I).

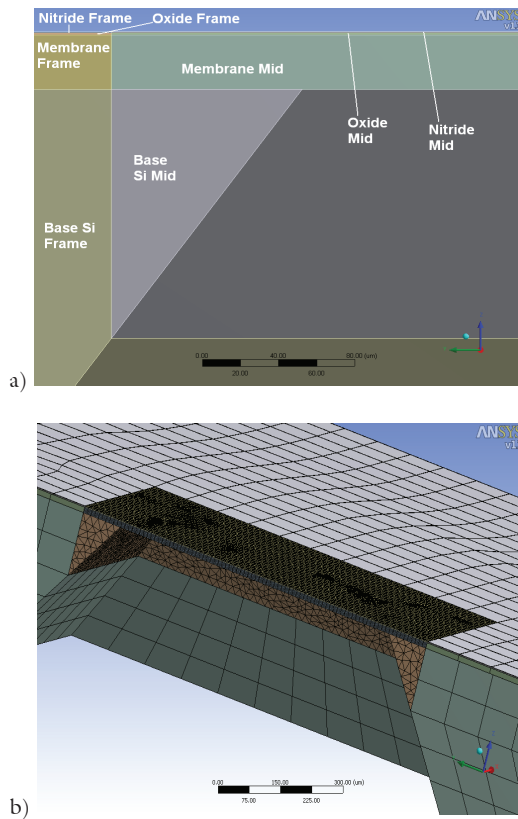


Figure.1: (a) Subdivision for the optimized mesh; (b) meshing overview

Table I. Anisotropic material properties of silicon.

$E_x$ [GPa]	$E_y$ [GPa]	$E_z$ [GPa]	$\nu_{xy}$	$\nu_{xz}$	$\nu_{yz}$
169.1	169.1	130.1	0.062	0.362	0.362

Fig. 2 shows the distributions of normal stresses  $\sigma_{xx}$ ,  $\sigma_{yy}$  and the shear stress  $\sigma_{xy}$ . In ideal case, at the resistor locations,  $\sigma_{xx}$  is equal to  $\sigma_{yy}$  and the shear stress is zero.

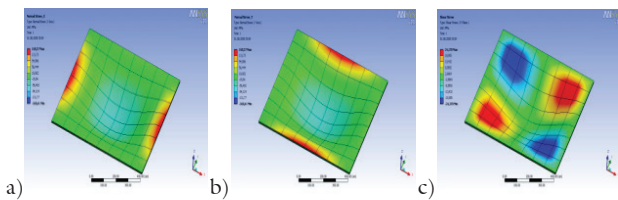


Figure 2. a) Normal stress  $\sigma_{xx}$ , b) normal stress  $\sigma_{yy}$ , c) shear stress  $\sigma_{xy}$

By a subsequent calculation with the corresponding physical relations for semiconductors [6] the conversion of stress distributions to electrical signals was done after the following simplified flow diagram shown in Fig. 3.

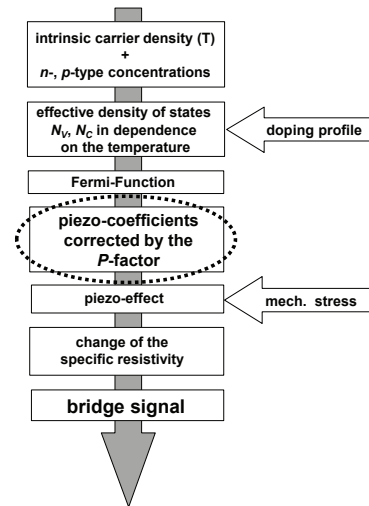


Figure.3 Signal evaluation flow; the dotted loop indicates the relevant step

The carrier concentration of the boron doped (*p*-type) resistors is determined by the boron concentration and the density of states in the conduction band. The probability of a charge carrier for the occupation of an allowed state is temperature dependent and described by the Fermi Function [6]. The impact of various carrier concentrations on the piezocoefficients and their temperature dependences was described by Kanda [4]. The dependencies of the relative piezocoefficients from the doping concentration and the temperature is shown in Fig. 4. These dependencies are crucial for the analyses of our pressure sensor systems. In the flow diagram shown in Fig. 3 the corresponding relevant step is accented by the dotted loop.

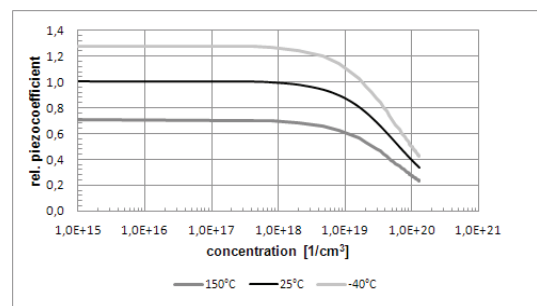
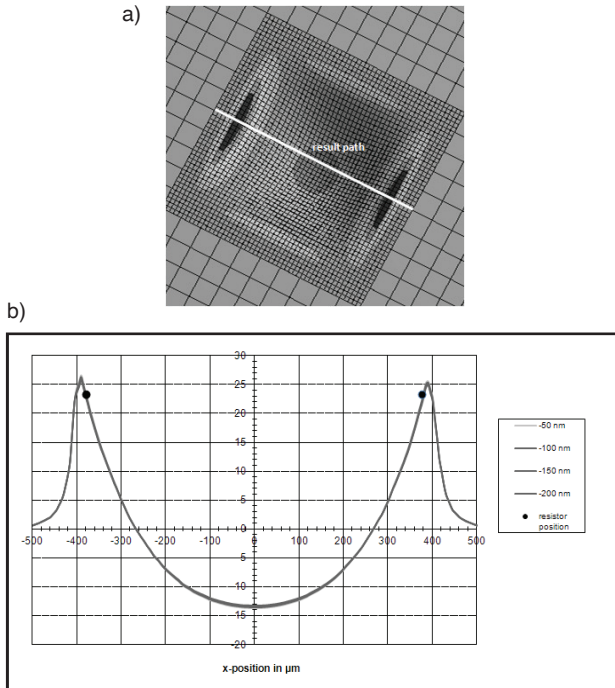


Figure.4 Relative piezocoefficients for *p*-doped silicon after [4] (see also [3])

As we know from the textbooks, the applied mechanical stress is altering the energetic positions of the allowed states within the conduction band, and with this leading to a variation of the specific resistivity. The variation of the resistivity is calculated for the geometric center of the resistor structure on the membrane. Four different result paths were taken at different *z*-coordinates (i.e. depths) within the membrane: at the surface, and at depths of 50, 100, 150, and 200 nm (Fig. 5a). For our analyses the average of these five stress values was taken as the effective applied stress value.

### III. RESULTS AND DISCUSSIONS



**Figure 5:** a) Position of the stress result path; b) stress values  $\sigma_{xx}$  (in MPa) for different depths in a 12  $\mu\text{m}$  membrane, i.e. with a 8  $\mu\text{m}$  thick Si membrane and a 4  $\mu\text{m}$  thick passivation layer

In a previous paper [1] the methodology was proven by measurements for a different membrane design for the two pressure ranges of 1 bar and 10 bar. In Fig. 6 the results for the 1-bar sensor type are shown. The membrane thicknesses were measured for all pressure sensors on a whole wafer, together with the according bridge signals. The measured signal values for certain membrane thickness values (11, 12, 13, 14, 15, 16  $\mu\text{m}$ ) were averaged, and the simulated values were laying within the standard deviation for these thicknesses. As can be seen from Fig. 6 there is a good correlation between the simulated values (dashed line) and the measured signals (solid line).

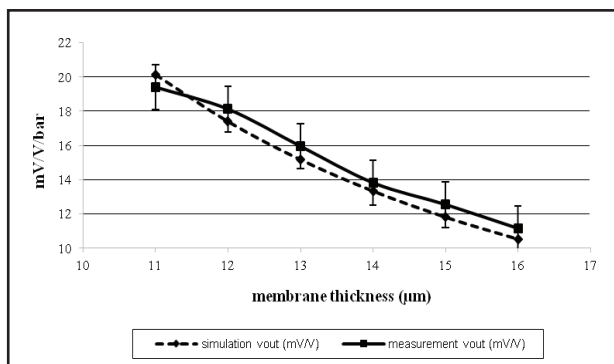


**Figure 6:** Method verification (see text)

Based on the verification study in [1], a new device initially designed for a nominal pressure range of 600 mbar is optimized for the lower pressure range down to 40 mbar without significant technological process variations as will be discussed next.

The studied integrated pressure sensor system (600 mbar device) with a membrane width of 800  $\mu\text{m}$  by 800  $\mu\text{m}$  has a target membrane thickness of 12  $\mu\text{m}$ . The standard passivation thickness of the membrane consists of an oxide-nitride layer compound of 4  $\mu\text{m}$ . The mechanical model was partitioned according to Fig. 1. Due to the symmetrical stress distributions in x- and y-direction, only  $\sigma_{xx}$  is derived from the FEA-result, and  $\sigma_{yy}$  is set equal to  $\sigma_{xx}$ . The stress values are taken along a path of different depths (i.e. at 50, 100, 150, 200 nm depth) across the mid of the membrane (Fig. 5b). The standard implantation procedure of the piezoresistors with a implantation dose (i.e. doping concentration) of about  $10^{20} \text{ cm}^{-3}$  results in a junction depth of around 200 nm, leading to no further contribution to piezoresistivity beyond that point. For this investigation, the different stress values over the different depths at the point of the geometric center of the resistor are averaged to 22 MPa (Fig. 5b). The black dot indicates the geometric position of the geometric center of the resistor structure on the membrane, 13  $\mu\text{m}$  away from the membrane rim.

**Table II.** Measured and simulated bridge signal for a 600 mbar load.

	Measured Value (20 parts)	Standard Deviation	Simulated value
Bridge Signal [mV/V]	4.44	0.44	4.56

In Table II the measured signals (i.e. averaged values are shown, which here based on twenty samples each) of the 600 mbar device are compared with the simulation results.

The on-chip signal conditioning circuitry was designed for a minimum bridge signal of about 2 mV/V [1]. Therefore, for lower nominal pressure ranges, the bridge signal of the studied device would decrease down to values which could not be amplified to achieve a feasible signal to noise ratio. Hence, the pressure system has to be modified, to reach this goal.

#### A. Mechanical Measures

To measure lower pressure values with a sufficient signal to noise ratio, two geometric parameters could be altered without changing the layout of the device: the membrane thickness (by a longer etching time) and the passivation layer thickness (by an additional back-etching of the passivation). The latter is necessary to shift the neutral phase of the membrane relatively more into the silicon part of a thinner membrane. A reasonable target thickness for the membrane is around 8  $\mu\text{m}$ , as this is producible in a standard wet etching process. If an 8  $\mu\text{m}$  Si-membrane with a 4  $\mu\text{m}$  passivation layer (total thick-

ness 12  $\mu\text{m}$ ) is bended, the neutral phase is located at a depth of 6  $\mu\text{m}$ , and with this only 2  $\mu\text{m}$  below the silicon surface. This situation results in the stress distribution along the membrane of the 600 mbar device, which is shown in Fig. 5. Due to deviations of the starting material (total thickness variation) and the etching process the membrane thickness might be lower than the target value, leading to a lower total thickness, probably with the position of the neutral phase at the depth of the piezoresistors. In this case no stress will occur at the resistors, and therefore, no signal is generated.

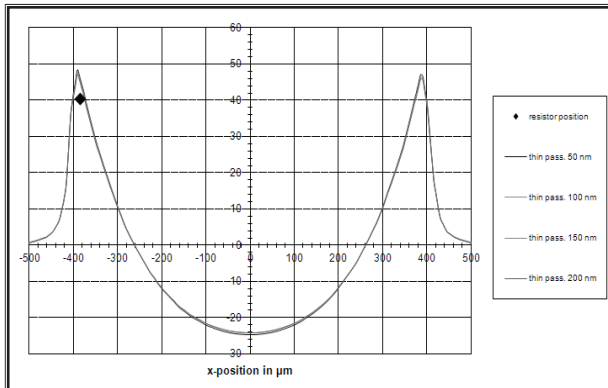


**Figure.7** Stress values  $\sigma_{xx}$  (in MPa) for different depths in a 12  $\mu\text{m}$  membrane with reduced passivation thickness

For the envisaged low pressure device, the new passivation thickness was lowered to 1.5  $\mu\text{m}$ ; and this measure alone raises the stress for the 12  $\mu\text{m}$  thick membrane, i.e. with a 10.5  $\mu\text{m}$  thick Si-membrane covered by the 1.5  $\mu\text{m}$  thick passivation layer, from 22 MPa (as shown in Fig. 5) to 40 MPa as can be seen in Fig. 7, if a 600 mbar pressure load is applied as before. This leads to the significantly increased simulated bridge signal of 8.3 mV/V. We can see that at the resistor positions the stress and the sensitivity are raised just by this simple change in the ration of the Si membrane thickness and the passivation layer thickness. In a linear approach the low end of the useful pressure range would be around 300 mbar resulting again in a reasonable signal, i.e. about 4.15 mV/V, and halving already the pressure range. Further improvements with regard to a much lower pressure range will be discussed in the next subchapter.

### B. Electrical Measures

A closer look at the signal evaluation steps shows an additional parameter, which can be altered to increase the piezoresistive bridge signal for a certain pressure load. According to the model of Kanda [4] a strong variation of the relative piezocoefficients occurs in dependence on the doping concentration. As can be seen in Fig. 6 showing the trend of the piezoresistive factor in dependence on the doping concentration in  $\text{cm}^{-3}$  (with the temperature as a parameter), the piezoresistive factor becomes

rather small for higher doping concentrations. The standard CMOS process used for the actual sensor pressure systems generates *p*-type piezoresistors with a boron concentration around  $1 \times 10^{20} \text{ cm}^{-3}$ . The dark black line (for  $T = 25^\circ\text{C}$ ) shows a relative piezoresistive factor for this doping concentration of about 0.4. A reduction of the doping concentration to about  $1 \times 10^{18} \text{ cm}^{-3}$  would increase the respective value of the relative piezocoefficient by a factor of 2.5, giving a 2.5 times higher bridge signal for the same stress value. Taking this into account the pressure sensor system can be optimized with regard to a significantly reduced pressure range with still very good signal-to-noise ratios.

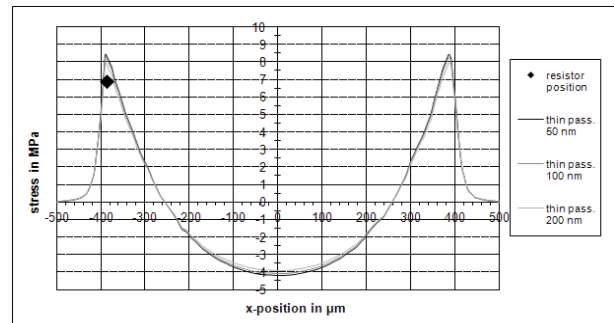


**Figure 8:** Stress values  $\sigma_{xx}$  for different depths in case of a 6  $\mu\text{m}$  membrane and a reduced doping concentration for the low pressure (40 mbar) device

The best results could be obtained up to now for the case documented in Fig. 8, where the stress distribution across a 6  $\mu\text{m}$  thick membrane topped with a 1.5  $\mu\text{m}$  thick passivation layer are shown for the quite low pressure load of 40 mbar. At this point it should be emphasized again that the overall membrane width (800  $\mu\text{m}$  by 800  $\mu\text{m}$ ) of the pressure sensor was not changed at all. The average stress over different depths at the geometric center position of the resistor is 6.9 MPa. The boron concentration for the piezoresistors was reduced here down to  $1.8 \times 10^{18} \text{ cm}^{-3}$  as compared to the standard value of  $1 \times 10^{20} \text{ cm}^{-3}$ . Table III shows the simulated and measured results (averaged over 40 samples). Again there is a good matching between the simulated and measured values.

**Table III.** Measured and simulated bridge signals for the modified sensor cell at 40 mbar pressure load.

	Measured Value (20 parts)	Standard Deviation	Simulated value
Bridge Signal [mV/V]	4.60	1.08	4.70

### IV. CONCLUSION

It has been shown, that a systematical approach for determining the electrical behavior of silicon based piezoresistive pressure sensor systems is successful. The developed method allows us to exactly determine and

tune the characteristics of pressure sensor systems to certain constraints, like fixed lateral outline of a membrane, by using real process parameters. These constraints always exist in the product development for mass production, as for cost efficiency a minimum number of masks of a product mask set should be changed for a maximum of applications. For a family of CMOS-integrated pressure sensor systems, this goal could be reached extending the low end pressure range from 600 mbar down to 40 mbar by just introducing a mask level for the implantation of the piezoresistors. As shown by verification, the method is reliable and its application for the modification of an existing sensor cells has led to the right process parameters without any additional technology run for iteration.

## REFERENCES

- [1] W. Schreiber-Prillwitz, M. Saukoski, G. Chmiel, and R. Job, "Design Approach and Realization of Integrated Silicon Piezoresistive Pressure Sensors for Wide Application Ranges", ECS Transactions, vol. 33, no. 8, 2010, 327-353.
  - [2] W. Schreiber-Prillwitz, M. Saukoski, G. Chmiel, and R. Job, "Development of a Robust Design for Wet Etched Cointegrated Pressure Sensor Systems", MRS Symposium Proceedings Series, vol. 1299, 2011, 129-134.
  - [3] W. Schreiber-Prillwitz, and R. Job, "Improvement of Integrated Pressure Sensor Systems Fabricated by a Combined CMOS- and MEMS-Technology with regard to Low Pressure Ranges", ECS Transactions, vol. 49, no. 1, 2012, 417-424.
  - [4] Y. Kanda, "A graphical representation of the piezoresistance coefficients in silicon", IEEE Transactions on Electron Devices, vol. ED-29, no. 1, 1982, 64-70.
  - [5] O. N. Tuffe, and E. L. Stelzer, "Piezoresistive Properties of Silicon Diffused Layers", Journal of Applied Physics, vol. 34, no. 2, 1963, 313-318.
  - [6] S. M. Sze, "Physics of Semiconductor Devices", 2<sup>nd</sup> edition, John Wiley and Sons, Inc., New York, 1981.
- \*) New address: TDK-EPC AG & Co. KG, 14532 Stahnsdorf, Germany